If the Sun is so quiet, why is the Earth ringing? A comparison of two solar minimum intervals

S. E. Gibson,[1] J. U. Kozyra,[2] G. de Toma,[1] B. A. Emery,[1] T. Onsager,[3] and B. J. Thompson[4]

Received 7 April 2009; revised 22 May 2009; accepted 26 June 2009; published 17 September 2009.

[1] Observations from the recent Whole Heliosphere Interval (WHI) solar minimum campaign are compared to last cycle's Whole Sun Month (WSM) to demonstrate that sunspot numbers, while providing a good measure of solar activity, do not provide sufficient information to gauge solar and heliospheric magnetic complexity and its effect at the Earth. The present solar minimum is exceptionally quiet, with sunspot numbers at their lowest in 75 years and solar wind magnetic field strength lower than ever observed. Despite, or perhaps because of, a global weakness in the heliospheric magnetic field, large near-equatorial coronal holes lingered even as the sunspots disappeared. Consequently, for the months surrounding the WHI campaign, strong, long, and recurring high-speed streams in the solar wind intercepted the Earth in contrast to the weaker and more sporadic streams that occurred around the time of last cycle's WSM campaign. In response, geospace and upper atmospheric parameters continued to ring with the periodicities of the solar wind in a manner that was absent last cycle minimum, and the flux of relativistic electrons in the Earth's outer radiation belt was elevated to levels more than three times higher in WHI than in WSM. Such behavior could not have been predicted using sunspot numbers alone, indicating the importance of considering variation within and between solar minima in analyzing and predicting space weather responses at the Earth during solar quiet intervals, as well as in interpreting the Sun's past behavior as preserved in geological and historical records.

Citation: Gibson, S. E., J. U. Kozyra, G. de Toma, B. A. Emery, T. Onsager, and B. J. Thompson (2009), If the Sun is so quiet, why is the Earth ringing? A comparison of two solar minimum intervals, *J. Geophys. Res.*, *114*, A09105, doi:10.1029/2009JA014342.

1. Introduction

[2] The three-dimensional structure of the solar wind is controlled and organized by the Sun's magnetic field, with a background (nontransient) component characterized by magnetic field lines having one footpoint attached to the Sun and the other open to interplanetary space. Such open magnetic field lines are generally believed to originate in coronal holes, and low-latitude coronal holes can be identified as sources of solar wind high-speed streams (HSS) at the Earth. When the solar wind magnetic field is southward, and thus antiparallel to the Earth's magnetic field, strong coupling between the magnetized plasma within these HSS and the Earth's magnetosphere results in flows of mass, momentum and energy into geospace from the solar wind. The solar wind velocity controls the rate at which its magnetic field is brought into contact with the Earth's magnetosphere, and, in general the energy input to geospace relates to both the solar wind velocity and the southward component of its magnetic field [*Kan and Lee*, 1979], and also on how long-lasting the stream is in its intersection with the Earth [*Maris and Maris*, 2005]. The key is the elevated level of solar wind magnetic field turbulence which triggers geospace activity that can continue for as long as it takes the stream to blow by the Earth [*Burlaga and Lepping*, 1977; *Tsurutani and Gonzalez*, 1987]. Moreover, HSS may return with each solar rotation as long as low-latitude coronal holes persist.

[3] In this paper we examine the origins and impact of HSS at the Earth during solar minimum using results from two international, interdisciplinary campaigns known as the Whole Sun Month (WSM) (10 August to 8 September 1996) and the Whole Heliosphere Interval (WHI) (20 March to 16 April 2008). We will provide context to this comparison by reviewing previous analyses that probe the physical properties involved from Sun to Earth, as well as recent observational studies that have begun to compare properties of the current solar minimum as compared to the last (note that these two minima are within the same Hale magnetic-polarity cycle). Our work is one of several past and current efforts to use these periods to characterize the three-dimensional interconnected solar-heliospheric-geospace system at

[1]High Altitude Observatory, National Center for Atmospheric Research, Boulder, Colorado, USA.
[2]Department of Atmospheric, Oceanic, and Space Sciences, University of Michigan, Ann Arbor, Michigan, USA.
[3]NOAA Space Weather Prediction Center, Boulder, Colorado, USA.
[4]NASA Goddard Space Flight Center, Greenbelt, Maryland, USA.

0148-0227/09/2009JA014342

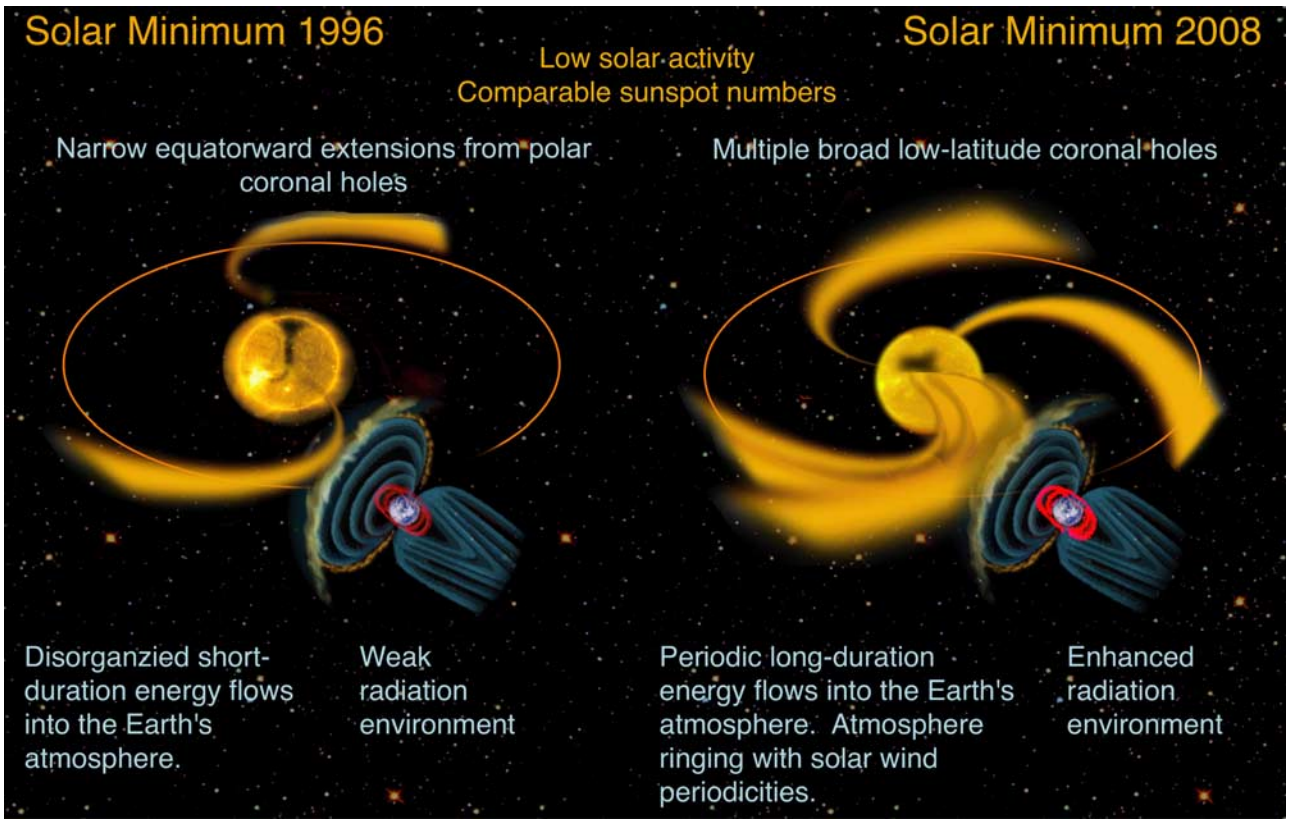

Figure 1. Overview of origins and impacts of high-speed streams (HSS) for two solar minima as observed during the WSM and WHI time periods (artist's conception). HSS are indicated in yellow, the solar coronal holes which are the sources of the Earth-intersecting HSS appear as dark regions on the central (yellow) images of the Sun, the Earth's magnetic fields are indicated in blue, and the radiation belts are indicated in red. Credit for the magnetosphere and solar images adapted as part of this illustration: NASA.

solar minimum [*Galvin and Kohl*, 1999, and references therein; *Chamberlin et al.*, 2009; *Lionello et al.*, 2009]. As we will describe below, the magnetic morphology at the Sun for the two campaigns were significantly different, with consequences extending to the Earth's space environment (see Figure 1 for an overview illustration). The absolute minimum of the current cycle has not yet been established, and cannot be until new cycle sunspots show a clear rise. However, as Figure 2 shows, by the time of the WHI campaign, sunspots had diminished to levels lower than last cycle minimum. The two intervals are thus comparably "quiet," and their differences illustrate the significant variation that may occur within and between solar minima.

2. Differences Between Solar Minima at the Sun and in the Solar Wind

[4] Observations at the Sun and in the solar wind, both above the poles and near the ecliptic plane, indicate differences between the current solar minimum and the last. Polar coronal holes appear smaller, and polar magnetic flux measured at the solar surface is 40% weaker this minimum relative to the last [*Kirk et al.*, 2009]. Magnetic fields measured in the solar wind above the Sun's poles [*Smith and Balogh*, 2008] are depleted by a similar amount (about a third), as are solar wind density (by 17–20%), and to a

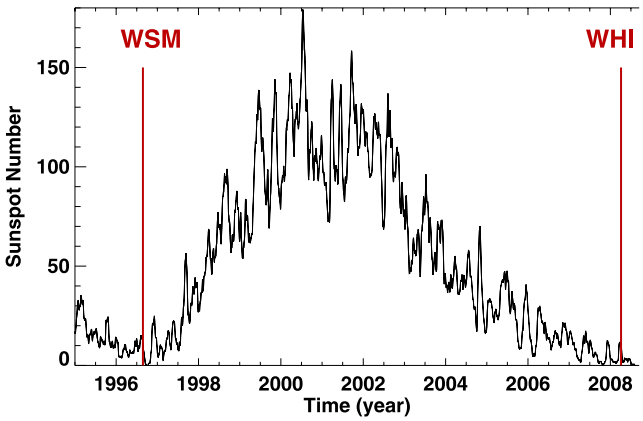

Figure 2. Sunspot number (27-day running average) from the last minimum to the present one, with red lines indicating WSM (10 August to 8 September 1996) and WHI (20 March to 16 April 2008). The sunspot number averaged over a solar rotation centered on WSM was 11.82, and over a rotation centered around WHI it was 11.00. For the nine solar rotations centered on these intervals (see Figure 5) the sunspot numbers averaged 8.75 (WSM) and 4.11 (WHI).

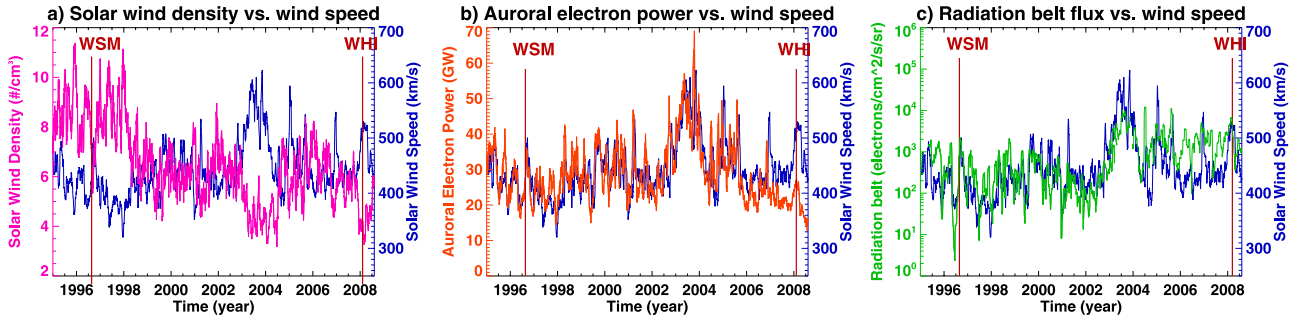

Figure 3. Observations putting WSM (10 August to 8 September 1996) and WHI (20 March to 16 April 2008) into solar cycle context. OMNI solar wind speed (indigo) is overlaid (a) with density (pink); (b) with combined NOAA-DMSP auroral electron power [*Emery et al.*, 2008] (orange); and (c) with >2 MeV outer radiation belt electron flux (green) (GOES 8: 1 May 1995 to 31 May 2003; GOES 10: 1 January 2003 to 31 December 2003; GOES 12: 1 January 2004 to 31 October 2008). The GOES satellite data were calibrated prelaunch and intercalibrated in flight when pairs of spacecraft operated at the same longitude [see *Wrenn*, 2008, and references therein]. All data have undergone a 27-day running average to highlight long-term trends.

lesser extent, velocity (≈3%) [*McComas et al.*, 2008; *Issautier et al.*, 2008]. Of considerable interest for space weather, differences between average solar minimum wind properties are also apparent in the vicinity of the Earth [*Owens et al.*, 2008; *Emery et al.*, 2009; *Lee et al.*, 2009]. As at the poles, average magnetic field strength near the Earth is lower (15% decreased), and, as Figure 3a illustrates, so is average solar wind density (45% decreased). However, Figure 3a also shows that the solar wind velocity near Earth has actually increased, by 13% on average. Note these and other ecliptic percent changes we present are based upon averages over nine solar rotations around WSM and WHI as shown in Figure 5.

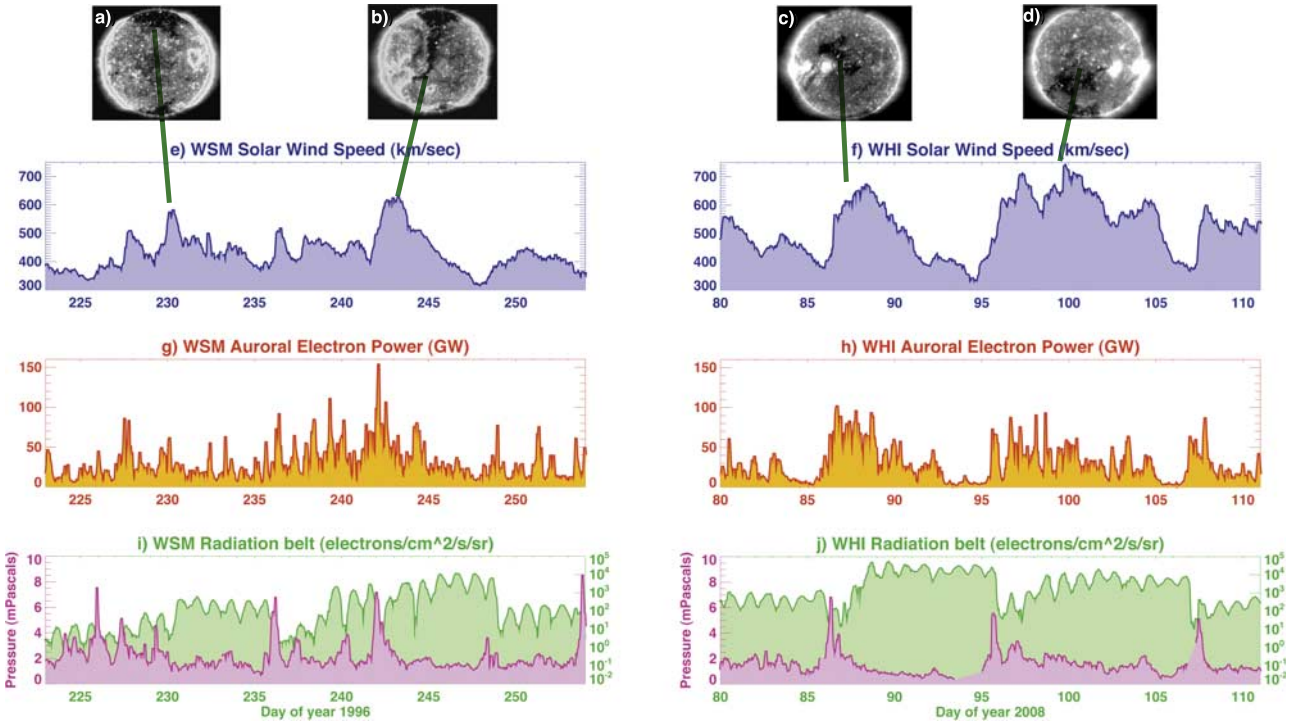

Figure 4. Low-latitude coronal holes and their associated high-speed solar wind streams during (a, b, e, g, i) WSM and (c, d, f, h, j) WHI. Figures 4a–4d show coronal holes in extreme-ultraviolet emission (SOHO/EIT): 12 August 1996, 26 August 1996, 25 March 2008, and 3 April 2008, respectively. Figures 4e and 4f show OMNI hourly solar wind velocity averages (indigo). Figures 4g and 4h show NOAA-DMSP auroral electron power (orange). Figures 4i and 4j show GOES 8 (WSM) and GOES 12 (WHI) >2 MeV outer radiation belt electron flux (green), with solar wind pressure (pink). A total of 31 days starting from 10 August 1996 (WSM) and 20 March 2008 (WHI) is plotted in Figures 4e–4j to account for a 4-day average wind travel time from the Sun.

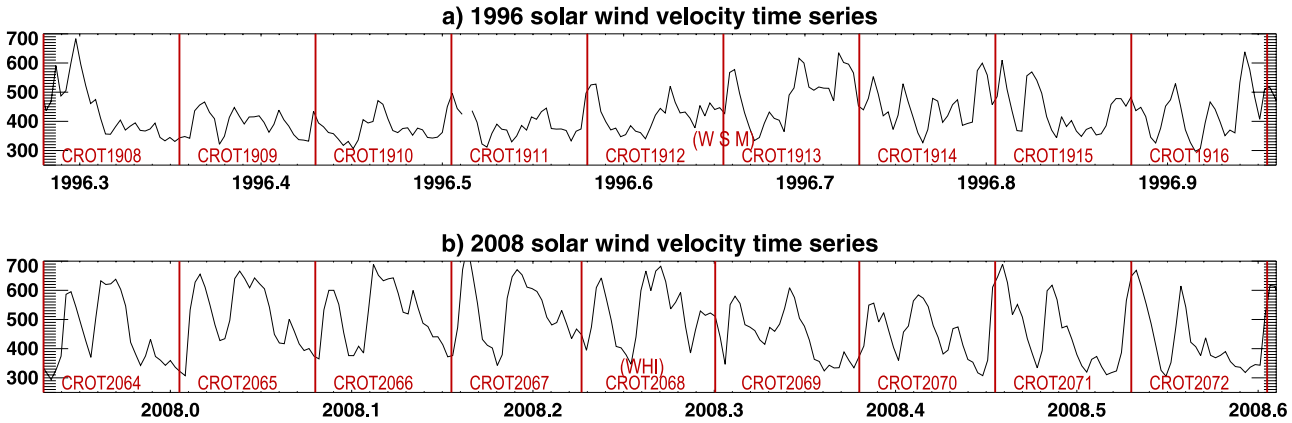

Figure 5. Time series of solar wind velocity for nine 27-day solar rotations surrounding (a) WSM and (b) WHI. Four days have been added to the solar rotation start times to account for travel time from Sun to Earth.

[5] A difference in global solar morphologies explains why the solar wind trends observed near the Earth differ from those observed above the solar poles. The solar minimum Sun is characterized by a strong polar magnetic field nearly aligned with its rotation axis, which leads to a solar wind emanating along polar magnetic field lines. This is a first-order approximation, however [*Luhmann et al.*, 2002], and the solar minimum corona during WHI had a more complex distribution of open magnetic flux at the Sun than it did during WSM. In particular, low-latitude coronal holes and thus fast wind sources occupied a larger fraction of near-equatorial latitudes during WHI than WSM (see Figures 1 and 4) [see also *Lee et al.*, 2009; *Tokumaru et al.*, 2009]. Because of the prevalence of low-latitude open flux this cycle compared to last, the percentage of time that Earth is engulfed in fast (≥450 km/s) solar wind increased from 31% to 55%, which explains the increased average solar wind velocity for the months surrounding WHI versus WSM. It also explains the larger decrease in solar wind density observed near Earth compared to above the Sun's pole, because HSS are rarified so that density and velocity are anticorrelated (Figure 3a).

[6] Figure 4 uses the WSM versus WHI periods to investigate how low-latitude open magnetic flux and resulting HSS differ between solar minima. During WSM, an elongated extension of the northern polar hole stretching below the equator (Figure 4b) was visible. However, a much larger fraction of solar longitudes were covered by low-latitude coronal holes during WHI (Figures 4c and 4d). As a result, the HSS during WHI were faster, longer-lasting, and generally more coherent than those during WSM (compare velocity plots in Figures 4e and 4f). Because the global morphology of the Sun did not change greatly in the solar rotations surrounding WHI, a pattern of two-three peaks in velocity tended to repeat (Figure 5b), leading to strong and distinct 9, 13.5, and 27-day periodicities (Figure 6). In

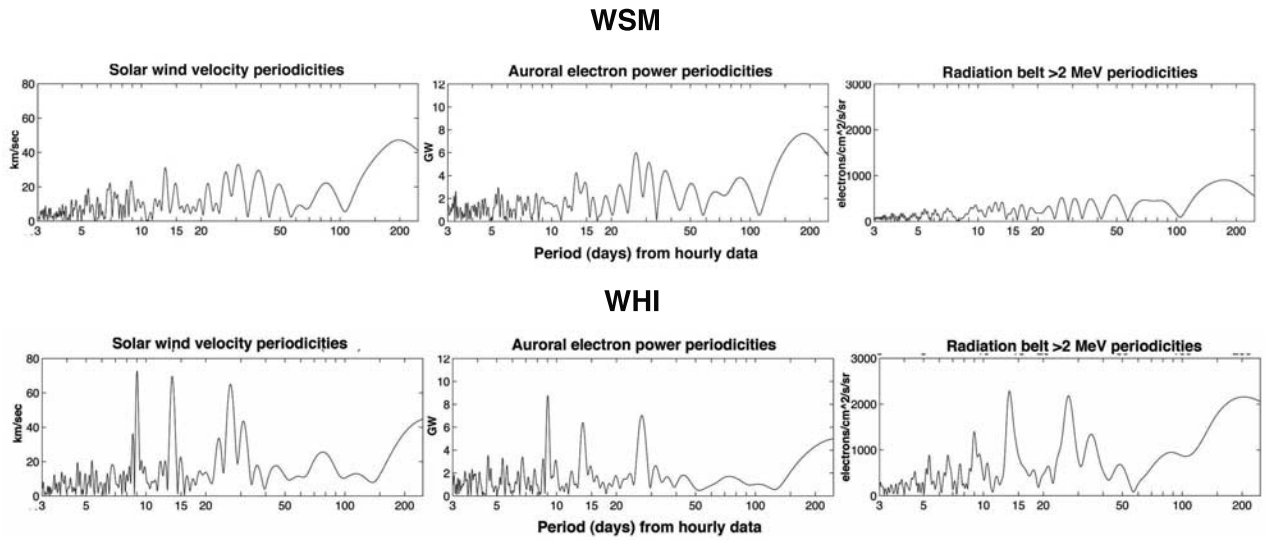

Figure 6. Analysis of the extended time periods centered on the WSM and WHI intervals shown in Figure 5, showing periodicities for solar wind velocity, auroral electron power, and >2 *MeV* outer radiation belt electron flux. Please see *Emery et al.* [2009] for further discussion of the wind velocity and auroral electron power periodicities and for details of the spectral analysis method.

contrast, the months surrounding WSM lacked a consistent pattern in the wind velocity time series (Figure 5a).

3. How These Differences Affect the Earth

[7] The arrival at Earth of each HSS during WSM and WHI corresponds to an increase in auroral power (compare Figures 4e and 4g and Figures 4f and 4h). Because the magnetic field associated with the second HSS in Figure 4h is pointed away from the Sun and WHI occurred in (northern hemisphere) spring, geometric effects resulted in a diminished amount of turbulent southward magnetic fields in the Earth's reference frame, and consequently an auroral power increase which does not reflect the length and strength of the associated HSS [*Russell and McPherron*, 1973; *Crooker*, 2000; *Vrsnak et al.*, 2007]. Figure 3b illustrates the generally strong correlation of auroral power and wind speed from last cycle minimum through the current minimum. However, the decreased magnetic field strength this cycle minimum results in a drop-off in the auroral power (orange) relative to the wind speed (indigo) in 2006–2008, because of the additional dependence of auroral power on magnetic field strength (see *Emery et al.* [2009] for a detailed discussion of the correlation factors of these quantities over several solar cycles). Thus, although HSS continue to drive auroral activity this minimum, the amplitudes of their associated turbulent magnetic fields are generally lower, resulting in diminished auroral power input overall (13% lower than last minimum). However, the recurrent HSS this minimum strongly modulate the auroral power, so the periodicities described above for solar wind velocity are apparent in auroral power this cycle minimum, and are quite different from the weak and broadly distributed auroral power modulations seen last cycle minimum (Figure 6).

[8] A particularly noticeable difference between the minima is the elevated radiation environment in geospace that persisted deep into solar minimum. Relativistic electrons form a torus that extends from 3–8 Earth radii, peaking at 4–5 Earth radii above the equator, which is referred to as the "outer radiation belt." High relativistic electron flux within this radiation belt can be a threat to the operation of satellites. Figure 3c shows that the flux of electrons greater than 2 MeV at 6–7 Earth radii above the equator (green) dropped steeply toward solar minimum in 1996, and, in fact, nearly disappeared around summer solstice of that year [*Li et al.*, 2001] (one and a half months before WSM began). However, the decline in the descending phase of the current cycle was relatively slow [*Wrenn*, 2008], and we show in Figure 3c that, even after sunspots and solar activity had dropped to levels lower than last minimum, radiation belt fluxes in the outer belt were still pumped up in association with continuing periodic HSS. For the months surrounding WHI, they were at levels on average 3.4 times higher (or 71% higher for a logarithmic comparison) than those surrounding WSM.

[9] The variations in the radiation environment surrounding the Earth are the result of a dynamic balance between sources and losses [*Reeves et al.*, 2003; *Green et al.*, 2004; *Onsager et al.*, 2007]. Observations indicate that the most important driver is solar wind speed, but for a strong radiation belt enhancement to develop, the high-speed wind must be accompanied by some southward component in the magnetic field turbulence it contains [*Blake et al.*, 1997; *Baker et al.*, 1998; *Miyoshi and Kataoka*, 2008]. This southward component triggers the periodic auroral activity thought to be essential for producing "seed" electrons, which are then accelerated to radiation belt energies over the course of 1–2 days [*Miyoshi et al.*, 2007]. This behavior can be seen in Figures 4i and 4j, where sustained peaks in >2 MeV electrons develop 1–2 days after the onset of HSS during both WSM and WHI. Note that the second HSS in WHI (between days 96 and 104) results in lower radiation belt flux than the first HSS (between days 86 and 90), despite the fact that wind speeds are higher and sustained longer in this stream: again, this is most likely due to the relative lack of southward magnetic fields.

[10] Radiation flux dropouts are observed to occur near the onset of HSS. Figures 4i and 4j show dropouts that coincide with solar wind pressure pulses and precede the major radiation belt enhancements in WSM and WHI. Recent statistical studies indicate that during flux dropout events the combination of high-speed solar wind and southward magnetic field drive a variety of processes in the Earth's magnetosphere that ultimately result in an overlap between regions of high-density cold and hot plasmas. Such regions may be the sites of intense plasma waves that scatter radiation belt electrons into the atmosphere and deplete outer belt fluxes in as little as 6 hours [*Borovsky and Denton*, 2009, and references therein].

[11] Figure 6 shows that the close causal connections between the HSS and the variations in radiation belt flux lead to 9, 13.5 and 27-day periodicities in the radiation belt flux data for WHI that closely parallel the behaviors already discussed for solar wind velocity and auroral power. As was also true for the wind velocity and auroral power, these periodicities are not evident in the WSM radiation belt data.

[12] The low values of auroral power this minimum introduces an interesting puzzle. During the last solar minimum, a similar drop in auroral power was met with a drop in radiation belt fluxes (Figures 3b and 3c). If the seed electrons are now at the low levels implied by the auroral power estimates, it raises the question of why the radiation belt fluxes have remained elevated. Recent studies indicate that low solar wind densities could lead to a number of effects that would diminish loss rates of both seed and relativistic electrons and thus enhance radiation belt fluxes [*Lyatsky and Khazanov*, 2008; *Borovsky and Denton*, 2009; *Kataoka and Miyoshi*, 2008]. Bearing in mind the complex nature of the coupled processes involved in the acceleration and depletion of radiation belt electron flux, it is likely that the enhanced levels in WHI relative to WSM are due to a combined geospace response to the relatively high solar wind speeds and low solar wind densities at the Earth, which in turn directly arise from the larger number of long-lived and repeating HSS.

4. Conclusions

[13] For months after sunspots reached levels lower than those of last cycle minimum, radiation in the Earth's outer belt remained at high levels and continued to ring with sustained and coherent activity having the 9-, 13.5- and 27-day periodicities characteristic of HSS in the solar wind. This was not observed in the last solar minimum and was

completely unanticipated. It is certainly possible that by the time the absolute minimum of the current cycle is established, the heliospheric magnetic morphology will have evolved into the predominantly dipolar configuration seen last cycle minimum. Even if not, and the current cycle minimum retains its more complex magnetic morphology, it is not possible to make claims that this solar minimum is "unusual" using a comparison of only two comprehensively observed cycles. What a comparison of the WSM and WHI campaign data does demonstrate, however, is that the distribution of low-latitude open magnetic flux on the Sun and subsequent structure in the solar wind is the key factor in determining how geospace will respond during times of low solar activity. Why low-latitude open magnetic flux and thus HSS at the Earth have been so prevalent this cycle minimum is not fully understood, but it may well relate to the overall weakening of the background solar wind [*Sheeley*, 2008; *Luhmann et al.*, 2009; *Tokumaru et al.*, 2009]. At the Earth, however, the consequence of a more complex solar magnetic morphology is distinct from that of a weak solar magnetic field. Indeed, for the outer radiation belt, the presence of multiple HSS overcomes the effects of a global decrease in solar wind magnetic field, which our current understanding would relate to diminished, rather than enhanced radiation belt relativistic electron flux.

[14] An increased level of HSS at solar minimum may have impacts that extend downward into the Earth's atmosphere. Periodicities in auroral, geomagnetic and atmospheric data, correlating to HSS and solar source periodicities, were also observed in the years leading up to the current solar minimum. HSS are known to peak during the declining phase of the solar cycle, and in 2003, intense HSS activity drove perturbations in the chemistry, dynamics, and energetics of the upper atmosphere [*Kozyra et al.*, 2006]. It came as a surprise when strong periodicities remained imprinted on a range of upper atmospheric quantities as the cycle moved toward solar minimum, a consequence of the HSS not dropping off as they had in previous cycles. These quantities include auroral and geomagnetic indices, thermospheric density and composition, ionospheric density, and daily global power radiated by nitric oxide (NO) and carbon dioxide (CO_2) in the thermosphere [*Temmer et al.*, 2007; *Vrsnak et al.*, 2007; *Crowley et al.*, 2008; *Emery et al.*, 2009; *Lei et al.*, 2008a, 2008b; *Mlynczak et al.*, 2008; *Thayer et al.*, 2008]. Preliminary analysis by J. Lei (private communication, 2008) shows a clear correlation between thermospheric neutral density and solar wind speed for the WHI interval, indicating the periodicities seen in the upper atmosphere during the descending phase of the solar cycle extend into the current solar minimum.

[15] The variation within and between solar minima has implications for analyzing and predicting space weather responses at the Earth during solar quiet intervals, and also for interpreting the Sun's past behavior as preserved in geological and historical records. If the low sunspot conditions of solar minima have analogies to conditions during solar "grand minima" (where sunspots all but disappear for extended periods), then HSS may introduce complexities to the Earth's response during these times as well. Indeed, it has been proposed that Earth-intersecting HSS were present during the Maunder minimum [1650–1715] [*Wang and Sheeley*, 2003]. The precise role that HSS played depends on interconnected and interacting processes both internal and external to the Earth's magnetosphere, and, as we have shown for the outer radiation belt, could even counter the effects of the lack of magnetic activity at the Sun. Determining the net impact of solar minimum differences on the Earth's atmosphere and space environment will require further coordinated, interdisciplinary modeling efforts to bring the pieces together.

[16] **Acknowledgments.** The Whole Heliosphere Interval (WHI) is coordinated under the auspices of the International Heliophysical Year, and we acknowledge David Webb's leadership role in WHI. We also thank the participants of the WHI Data and Modeling Assessment Workshop (August 2008, Boulder, Colorado) for working group discussions and P. Riley for showing us early model results for WHI that helped frame our understanding of the system. OMNI solar wind and IMF data include Wind and ACE satellite data time-shifted to the Earth's magnetosphere. The intercalibrated NOAA and DMSP auroral electron powers are from the CEDAR Database, which is supported by the NSF. SOHO is a project of international collaboration between ESA and NASA. G.d.T.'s work was supported by NASA-LWS grant NNH05AA49I, B.A.E.'s work was supported by NASA-LWS grant NNH05AB54I, and J.U.K.'s work was supported by NASA-SRT grants NNG05GM48G, NNX08AQ15G, and NNX08AV83G. NCAR is sponsored by the NSF.

[17] Amitava Bhattacharjee thanks Antoinette Galvin and Bojan Vrsnak for their assistance in evaluating this paper.

References

Baker, D. N., X. Li, J. B. Blake, and S. G. Kanekal (1998), Strong electron acceleration in the Earth's magnetosphere, *Adv. Space Res.*, *21*, 609–613.

Blake, J. B., D. N. Baker, N. Turner, K. W. Ogilvie, and R. P. Lepping (1997), Correlation of changes in the outer-zone relativistic-electron population with upstream solar wind and magnetic field measurements, *Geophys. Res. Lett.*, *24*, 927–929.

Borovsky, J. E., and M. H. Denton (2009), Relativistic-electron dropouts and recovery: A superposed-epoch study of the magnetosphere and the solar wind, *J. Geophys. Res.*, A02201, doi:10.1029/2008JA013128.

Burlaga, L. F., and R. P. Lepping (1977), The causes of recurrent geomagnetic storms, *Planet. Space Sci.*, *25*, 1151.

Chamberlin, P. C., T. N. Woods, D. A. Crotser, F. G. Eparvier, R. A. Hock, and D. L. Woodraska (2009), Solar cycle minimum measurements of the solar extreme ultraviolet spectral irradiance on 14 April 2008, *Geophys. Res. Lett.*, *36*, L05102, doi:10.1029/2008GL037145.

Crooker, N. (2000), Solar and heliospheric geoeffective disturbances, *J. Atmos. Sol. Terr. Phys.*, *62*, 1071–1085.

Crowley, G., A. Reynolds, J. P. Thayer, J. Lei, L. J. Paxton, A. B. Cristensen, Y. Zhang, R. R. Meier, and D. J. Strickland (2008), Periodic modulations in thermospheric composition by solar wind high speed streams, *Geophys. Res. Lett.*, *35*, L21106, doi:10.1029/2008GL035745.

Emery, B. A., V. Coumans, D. S. Evans, G. A. Germany, M. S. Greer, E. Holeman, K. Kadinsky-Cade, R. J. Rich, and W. Xu (2008), Seasonal, Kp, solar wind, and solar flux variations in long-term single-pass satellite estimates of electron and ion auroral hemispheric power, *J. Geophys. Res.*, *113*, A06311, doi:10.1029/2007JA012866.

Emery, B. A., I. G. Richardson, D. S. Evans, R. J. Rich, and W. Xu (2009), Solar wind structure sources and periodicities of global electron hemispheric power over three solar cycles, *J. Atmos. Sol. Terr. Phys.*, *71*, 1157–1175, doi:10.1016/j.jastp.2008.08.005.

Galvin, A. B., and J. B. Kohl (1999), Whole sun month at solar minimum: An introduction, *J. Geophys. Res.*, *104*, 9673–9678.

Green, J. C., T. G. Onsager, T. P. O'Brien, and D. N. Baker (2004), Testing loss mechanisms capable of rapidly depleting relativistic electron flux in the Earth's outer radiation belt, *J. Geophys. Res.*, *109*, A12211, doi:10.1029/2004JA010579.

Issautier, K., G. M.-V. N. Le Chat, M. Moncuquet, S. Hoang, R. J. MacDowall, and D. J. McComas (2008), Electron properties of high-speed solar wind from polar coronal holes obtained by Ulysses thermal noise spectroscopy: Not so dense, not so hot, *Geophys. Res. Lett.*, L19101, doi:10.1029/2008GL034912.

Kan, J. R., and L. C. Lee (1979), Energy coupling function and solar wind-magnetosphere dynamo, *Geophys. Res. Lett.*, *6*, 577–580.

Kataoka, R., and Y. Miyoshi (2008), Magnetosphere inflation during the recovery phase of geomagnetic storms as an excellent magnetic confinement of killer electrons, *Geophys. Res. Lett.*, *35*, L06S09, doi:10.1029/2007GL031842.

Kirk, M. S., W. D. Pesnell, C. A. Young, and S. A. Hess Webber (2009), Automated detection of EUV polar coronal holes during solar cycle 23, *Sol. Phys.*, *257*, 99–112, doi:10.1007/s11207-009-9369-y.

Kozyra, J. U., et al. (2006), Response of the upper/middle atmosphere to coronal holes and powerful high-speed solar wind streams in 2003, in *Recurrent Magnetic Storms: Corotating Solar Wind Streams*, *Geophys. Monogr. Ser.*, vol. 167, edited by B. Tsurutani et al., pp. 319–340, AGU, Washington, D. C.

Lee, C. O., J. G. Luhmann, X. P. Zhao, Y. Liu, P. Riley, C. N. Arge, C. T. Russell, and I. de Pater (2009), Effects of the weak polar fields of solar cycle 23: Investigation using OMNI for the STEREO mission period, *Sol. Phys.*, *256*, 345–363, doi:10.1007/s11207-009-9345-6.

Lei, J., J. P. Thayer, J. M. Forbes, E. K. Sutton, R. S. Nerem, M. Temmer, and A. M. Veronig (2008a), Global thermospheric density variations caused by high-speed solar wind streams during the declining phase of solar cycle 23, *J. Geophys. Res.*, *113*, A11303, doi:10.1029/2008JA013433.

Lei, J., J. P. Thayer, J. M. Forbes, Q. Wu, C. She, W. Wan, and W. Wang (2008b), Ionosphere response to solar wind high-speed streams, *Geophys. Res. Lett.*, *35*, L19105, doi:10.1029/2008GL035208.

Li, X., D. N. Baker, S. G. Kanekal, M. Looper, and M. Temerin (2001), Long term measurements of radiation belts by sampex and their variation, *Geophys. Res. Lett.*, *28*, 3820–3827.

Lionello, R., J. A. Linker, and Z. Mikic (2009), Multispectral emission of the Sun during the first whole Sun month, *Astrophys. J.*, *690*, 902, doi:10.1088/0004-637X/690/1/902.

Luhmann, J. G., Y. Li, C. N. Arge, P. R. Gazis, and R. Ulrich (2002), Solar cycle changes in coronal holes and space weather cycles, *J. Geophys. Res.*, *107*(A8), 1154, doi:10.1029/2001JA007550.

Luhmann, J. G., C. O. Lee, Y. Li, C. N. Arge, A. B. Galvin, K. Simunac, C. T. Russell, R. A. Howard, and G. Petrie (2009), Solar wind sources in the late declining phase of cycle 23: Effects of the weak solar polar field on high speed streams, *Sol. Phys.*, *256*, 285–305, doi:10.1007/s11207-009-9354-5.

Lyatsky, W., and G. V. Khazanov (2008), Effect of geomagnetic disturbances and solar wind density on relativistic electrons at geostationary orbit, *J. Geophys. Res.*, *113*, A08224, doi:10.1029/2008JA013048.

Maris, O., and G. Maris (2005), Specific features of the high-speed plasma stream cycles, *Adv. Space Res.*, *35*, 2129–2140.

McComas, D. J., R. W. Ebert, H. A. Elliott, B. E. Goldstein, J. T. Gosling, N. A. Schwadron, and R. M. Skoug (2008), Weaker solar wind from the polar coronal holes and the whole Sun, *Geophys. Res. Lett.*, *35*, L18103, doi:10.1029/2008GL034896.

Miyoshi, Y., and R. Kataoka (2008), Probabilistic space weather forecast of the relativistic electron flux enhancement at geosynchronous orbit, *J. Atmos. Sol. Terr. Phys.*, *70*, 475–481.

Miyoshi, Y., A. Morioka, R. Kataoka, Y. Kasahara, and T. Mukai (2007), Evolution of the outer radiation belt during the November 1993 storms driven by corotating interaction regions, *J. Geophys. Res.*, *112*, A05210, doi:10.1029/2006JA012148.

Mlynczak, M. G., et al. (2008), Solar-terrestrial coupling evidenced by periodic behavior in geomagnetic indexes and the infrared energy budget of the thermosphere, *Geophys. Res. Lett.*, *35*, L05808, doi:10.1029/2007GL032620.

Onsager, T. G., J. C. Green, G. D. Reeves, and H. J. Singer (2007), Solar wind and magnetospheric conditions leading to the abrupt loss of outer radiation belt electrons, *J. Geophys. Res.*, *112*, A01202, doi:10.1029/2006JA011708.

Owens, M. J., N. U. Crooker, N. A. Schwadron, T. S. Horbury, S. Yashiro, H. Xie, O. C. St. Cyr, and N. Gopalswamy (2008), Conservation of solar magnetic flux and the floor in the heliospheric magnetic field, *Geophys. Res. Lett.*, *35*, L20108, doi:10.1029/2008GL035813.

Reeves, G. D., K. L. McAdams, R. H. W. Friedel, and T. P. O'Brien (2003), Acceleration and loss of relativistic electrons during geomagnetic storms, *Geophys. Res. Lett.*, *30*(10), 1529, doi:10.1029/2002GL016513.

Russell, C., and R. McPherron (1973), Semiannual variation of geomagnetic activity, *J. Geophys. Res.*, *78*, 92–108.

Sheeley, N. R., Jr. (2008), A century of polar faculae variations, *Astrophys. J.*, *680*, 1553.

Smith, E. J., and A. Balogh (2008), Decrease in heliospheric magnetic flux in this solar minimum: Recent Ulysses magnetic field observations, *Geophys. Res. Lett.*, L22103, doi:10.1029/2008GL035345.

Temmer, M., B. Vrsnak, and A. M. Veronig (2007), Periodic appearance of coronal holes and the related variation of solar wind parameters, *Sol. Phys.*, *241*, 371–383, doi:10.1007/s11207-007-0336-1.

Thayer, J. P., J. Lei, J. M. Forbes, E. K. Sutton, and R. S. Nerem (2008), Thermospheric density oscillations due to periodic solar wind high-speed streams, *J. Geophys. Res.*, *113*, A06307, doi:10.1029/2008JA013190.

Tokumaru, M., M. Kojima, K. Fujiki, and K. Hayashi (2009), Non-dipolar solar wind structure observed in the cyce 23/24 minimum, *Geophys. Res. Lett.*, L09101, doi:10.1029/2009GL037461.

Tsurutani, B., and W. Gonzalez (1987), The cause of high-intensity long-duration continuous AE activity (HILDCAAs): Interplanetary Alfven wave trains, *Planet. Space Sci.*, *35*, 405–412.

Vrsnak, B., M. Temmer, and A. Veronig (2007), Coronal holes and the solar wind high-speed streams: II. Forecasting the geomagnetic effects, *Sol. Phys.*, *240*, 331.

Wang, Y.-M., and N. R. J. Sheeley (2003), Role of the Sun's non-axisymmetric open flux in cosmic-ray modulation, *Astrophys. J.*, *591*, 1248.

Wrenn, G. L. (2008), Chronology of killer electrons: Solar cycles 22 and 23, *J. Atmos. Sol. Terr. Phys*, *71*, 1210–1218, doi:10.1016/j.jastp.2008.08.002.

G. de Toma, B. A. Emery, and S. E. Gibson, High Altitude Observatory, National Center for Atmospheric Research, P.O. Box 3000, Boulder, CO 80307, USA. (sgibson@ucar.edu)

J. U. Kozyra, Department of Atmospheric, Oceanic, and Space Sciences, University of Michigan, Space Research Building, 2455 Hayward Street, Ann Arbor, MI 48109-2143, USA.

T. Onsager, NOAA Space Weather Prediction Center, W/NP9, 325 Broadway, Boulder, CO 80305, USA.

B. J. Thompson, NASA Goddard Space Flight Center, 8800 Greenbelt Road, Greenbelt, MD 20771, USA.